Delgard et al (2012) Hydrob 699 69-84

DATASET · OCTOBER 2013

7 AUTHORS, INCLUDING:

B. Deflandre
University of Bordeaux
78 PUBLICATIONS **611** CITATIONS
SEE PROFILE

Edouard Metzger
University of Angers
73 PUBLICATIONS **568** CITATIONS
SEE PROFILE

Donald B. Nuzzio
Analytical Instrument Systems, Inc.
37 PUBLICATIONS **1,085** CITATIONS
SEE PROFILE

Sylvain Capo
Telespazio
44 PUBLICATIONS **185** CITATIONS
SEE PROFILE

Hydrobiologia (2012) 699:69–84
DOI 10.1007/s10750-012-1154-5

COASTAL LAGOON ECOSYSTEMS

In situ study of short-term variations of redox species chemistry in intertidal permeable sediments of the Arcachon lagoon

M. L. Delgard · B. Deflandre · E. Metzger · D. Nuzzio · S. Capo · A. Mouret · P. Anschutz

Published online: 10 July 2012

Abstract We investigated the composition of porewaters in intertidal sediments in response to the diurnal rise and fall of tides. For this reason, we deployed an in situ voltammetric system to measure vertical distribution and time-series at defined depths of O_2, Mn(II), Fe(II), and S(−II) in the porewater of permeable sediments from a protected beach in the Arcachon Bay. We also report microprofiles of O_2 and pH together with sediment properties (organic carbon, particulate reactive manganese and iron, porosity and permeability). Results shows that the oxygen dynamics in the upper sediment at low tide appeared to be mainly controlled by microphytobenthos activity, which may migrate downward just before immersion. The tidal forcing seemed to influence the oxygen dynamic in a minor way through flushing of the uppermost sediment porewater layer at the beginning and end of immersion. Vertical profiles and time-series measurements showed that the distributions of reduced species varied with tides. Although this work reveals that the upper sediment layer was subject to redox changes, the response of vertical distributions of redox species to tidal and night–day cycles did not have a cyclic pattern.

Keywords Benthic biogeochemistry · Intertidal flat · Permeable sediment · In situ voltammetry · Tidal pumping

Guest editors: R. de Wit, N. Mazouni & P. Viaroli / Research and Management for the Conservation of Coastal Lagoon Ecosystems: South – North Comparisons

M. L. Delgard · B. Deflandre (✉) · S. Capo · A. Mouret · P. Anschutz
UMR CNRS 5805 EPOC, University of Bordeaux 1, Av. des Facultés, 33400 Talence, France
e-mail: b.deflandre@epoc.u-bordeaux1.fr

B. Deflandre
UMR CNRS 7578, Institut de Physique du Globe de Paris & Université Paris 7, Paris, France

E. Metzger
Laboratoire de Bio-Indicateurs Actuels et Fossiles, University Angers, 2 bd Lavoisier, 49045 Angers Cedex 01, France

D. Nuzzio
Analytical Instrument Systems Inc., 118 Old York Road, Ringoes, NJ O8551, USA

Introduction

Coastal lagoons are among the most productive environments of the ocean (Falkowski et al., 1998). Several studies have considered complex interactions between chemical and biological processes in coastal lagoons. For example, the impact of seagrass on the sediment biogeochemistry and associated fauna has been well documented (Viaroli et al., 1996; Azzoni et al., 2001; de Wit et al., 2001; Nielsen et al., 2001; Blanchet et al., 2004; Deborde et al., 2008a). Recent

studies have also focused on biogeochemical processes in intertidal areas (Pringault et al., 1999; Böttcher et al., 2000; Jahnke et al., 2003; Billerbeck et al., 2006a, b; Deborde et al., 2008b; Rauch & Denis, 2008). However, reports on the influence of tidal cycles on the vertical distributions of redox species in intertidal sediments are sparse (Rocha & Cabral, 1998; Taillefert et al., 2007; Jansen et al., 2009).

It is well known that the tidal forcing generates transports of particulate and dissolved materials in permeable intertidal sediments (Huettel et al., 1998; Rusch & Huettel, 2000; Rusch et al., 2000). These advective processes concern the surface sediment (Rocha, 1998; Rusch et al., 2001) as well as the deep layers (Beck et al., 2008; Deborde et al., 2008b). Billerbeck et al. (2006b) suggested that two types of porewater transport may occur in intertidal permeable sediments. The first process is a slow 'body circulation' that would affect deeper sediment layers during low tide, implying longer flow paths and porewater residence times. This is likely driven by a pressure gradient between the porewater level and the low water level during ebb. The second process, termed as the 'skin circulation', is proposed to affect the uppermost sediment layer during inundation. It would be characterized by shorter flow paths and residence times with an immediate feedback to ecosystem (Billerbeck et al., 2006b; Jansen et al., 2009). Thus, these complex processes of water circulation in the permeable sediments may affect the vertical distributions of redox species in response to the tidal cycles.

Deborde et al. (2008b) demonstrated in the Arcachon Bay that the tidal pump generates a seeping of anoxic mudflat porewaters during ebb and an advection of porewaters in permeable sediments, becoming a major contributor of nutrient export to the water column. Based on an ex situ approach (i.e., sampling from sediment cores), this work clearly showed the effect of tidal forcing on the chemical composition of creeks at large spatial and temporal scales. However, transport mechanisms at small scales were not considered because traditional ex situ approaches that have been used to study biogeochemistry of the Arcachon Bay tidal flat are not suitable to study rapid variations of the porewater chemistry at small spatial scales (Taillefert et al., 1999, 2007; Jansen et al., 2009).

Improving our understanding of the impact of tidal forcing on the biogeochemistry of permeable sediment thus requires multiple observations and quantifications of short-term variations of the sediment redox chemistry with a high spatial and temporal resolution. This is possible with in situ deployments of microelectrodes (Taillefert et al., 1999). Mono-specific microsensors were used in situ for O_2 or sulfide measurements in permeable sediments over whole tidal cycles (e.g. De Beer et al., 2005; Billerbeck et al., 2006a, b; Roy et al., 2008; Jansen et al., 2009). A voltammetric Au/Hg microelectrode developed by Brendel & Luther (1995) enabled to measure, simultaneously and in situ, the vertical distributions of several redox chemical species involved in diagenetic processes from continental margin sediments (e.g., Luther et al., 1999; Reimers et al., 2004) to deep-sea hydrothermal vents (e.g., Luther et al., 2001 More recently, Taillefert et al. (2007) used this innovative in situ voltammetric approach in salt marsh sediments (Skidaway, Georgia, USA), showing that tides drastically influenced the vertical distributions of redox species in intertidal salt marsh sediments, and yet characterized by low permeability.

In this article, we present results from in situ measurements of vertical distributions and time-series at defined depths of O_2, Mn(II); Fe(II) and S(−II) obtained with an innovative voltammetric system in an permeable sediment of the Arcachon lagoon. The voltammetric measurements were associated with microprofiles of O_2 and pH, and with sediment solid phase properties. The objective was to investigate in situ the short-term variations of the vertical distribution of key redox species [O_2, Mn(II), Fe(II), S(−II)] in response to the tidal and diurnal cycles in order to document the role of tidal forcing on the biogeochemistry of permeable sediments from the Arcachon lagoon.

Materials and methods

Study site

The Arcachon Bay is a mesotidal, shallow lagoon of 180 km^2, located on the French Atlantic coast (44°40′N, 1°10′W; Fig. 1). The tide is semi-diurnal, with an amplitude from 1.1 to 4.9 m (Gassiat, 1989). At low tide, in the inner lagoon (156 km^2), tidal channels drain large tidal flats (115 km^2). At high tide, surface water temperature fluctuates annually between 1 and 25°C, and surface water salinity between 22 and

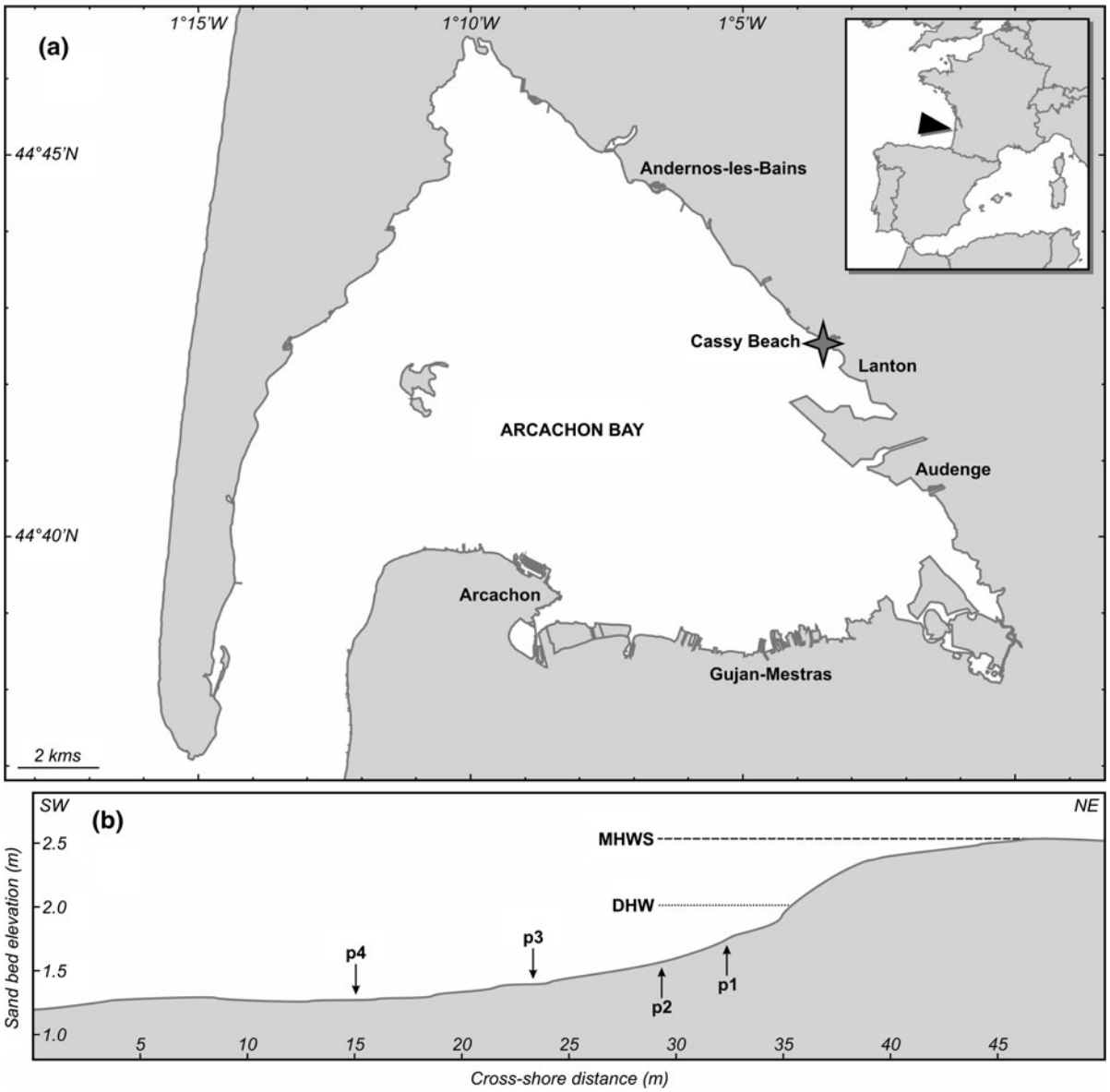

Fig. 1 **a** Map of the Arcachon Bay. **b** Topographic profile of the Cassy Beach indicating the 'cross-shore' transect used in this work. *Arrows* represent the sites used for measurements. Mean high water level during spring tides (MHWS) and daily high water level (DHW) are indicated

32 (Deborde et al., 2008a). The landward part of the bay is affected by moderate river input and underground freshwater discharge (Rimmelin et al., 1998; Canton et al., 2010). The lower part of the intertidal zone consists of muddy sediments (grain size: 15–40 μm), whereas the upper parts are made of permeable, sandy sediments (grain size: ∼250 μm). Permeable, sandy sediments also crop out in the beds of the largest channels (Deborde et al., 2008b).

The study site is located on a sloping sand flat (2.5 cm m^{-1}) in the southeast portion of Arcachon Bay (Fig. 1). The beach is covered for ∼3 h during high tide. Measurements were performed in the lower part of the beach, where the sediment remained saturated with water at high and low tides. Salinity of the water was about 24 and the temperature varied from 14 to 18°C. The sediment consists of slightly silty (median grain size = 360 μm in the first centimeter; measured

with a Malvern masterized laser granulometer) and permeable sand (1.2×10^{-11} m^2; measured with a permeameter according to the Darcy law).

Sampling strategy

The vertical distribution of redox species of the studied area was characterized from vertical profiles performed with various in situ/ex situ approaches at several sites, P1–P4, located on a beach along a cross-shore gradient of about 20-m long (Fig. 1). Porewater composition was characterized in situ with voltammetric, Clark-type and pH sensors at sites P1, P2, and P4 on April 30, 2009. Sediment cores were collected in P2, P3, and P4 for additional analysis of the solid phase just after in situ profiling. Then, we used two different approaches based on in situ methodologies to characterize the short-term evolution of the sediment biogeochemistry. The first approach consisted of successive depth profiling over tidal cycles with voltammetric and Clark-type oxygen sensors at site P3 on April 7 and 8, 2009. The next day, continuous recordings of the composition of porewaters (time-series) were measured at the same site P3, at six fixed depths in the sediment with voltammetric sensors during 20 h.

Methods

Voltammetric measurements

Voltammetric measurements were obtained in situ with mercury-plated, gold (Au/Hg) microelectrodes. A three-electrode voltammetric system was used to measure dissolved O_2, Fe(II), Mn(II), and S(−II) (i.e., $H_2S + HS^- + S^{-2}$, hereafter referred as $\sum H_2S$) concentrations, and to detect the presence of soluble Fe(III) and FeS molecular clusters (Brendel & Luther, 1995). The system consists of an Ag/AgCl reference electrode, the Au/Hg working electrode, and a Pt counter electrode, which is connected to a computer-operated DLK-100A potentiostat (Analytical Instrument Systems Inc., AIS). In situ voltammetric measurements were performed with a 50-m long cable (AIS) equipped with an amplifier, linking the electrodes to the potentiostat on the coast. Up to eight working electrodes were bundled together and scanned sequentially at each depth using a DLKMUX-1 electrode multiplexer (AIS).

In situ depth-profiles were conducted continuously over whole tidal cycles, with a lander equipped with a remotely controlled micromanipulator. For these measurements, a working electrode was pushed down with vertical increments varying from 500 μm close to the surface to 1 cm below 9 cm depth. The position of the SWI was estimated visually at low tide, or at high tide, based on the abrupt decrease observed in the voltammetric noise upon reaching the sediment surface. In situ time-series data were collected using up to six gold amalgam electrodes (EP2–EP7) positioned at different depths in the sediment. Sensors EP2 and EP3 were positioned 2 mm above the SWI and 7 mm below the SWI, respectively. Sensor EP2 recorded measurements only at high tide when the three-electrode system was closed (i.e., working, counter and reference electrodes). Two other sensors were placed in the suboxic zone, but they stopped running 1 h after the beginning of measurements because of a problem with waterproofing. The last two electrodes, EP6 and EP7, were placed at depths of 82 and 107 mm in the layer where sulfide was always detected throughout the depth-profile measurements. The electrodes were inserted using a solid plastic vertical holder in such a way that measurements were performed in the undisturbed sediments. However, the possibility that the vertical holder may have affected the local porewater circulation is not excluded.

Two types of gold amalgam working electrodes were manufactured, as previously described by Luther et al. (2008). Glass microelectrodes were used for depth profiling, whereas polyethyletherketone (PEEK) electrodes were specifically used for the time-series. Glass working microelectrodes were fabricated from a hollow glass tube pulled at one end under high temperature to form a tip of 0.5–1 mm in diameter and 3–5 cm in length. A 100-μm gold wire was sealed in the glass tip with an epoxy resin (West System) and contacted to the wire of a coaxial cable with Ag solder. PEEK working electrodes were built in the same way, encasing the gold wire in PEEK tubing. To ensure a waterproof seal, the top end of both kinds of working (micro)electrodes were coated with Scotchkote (3 M) electrical coating and Scotchfil (3 M) electrical insulation putty. Once constructed, each electrode tip was sanded with grit paper and polished successively with

Fig. 2 Depth profiles of O_2, Fe(II), Mn(II), $\sum H_2S$, FeS(aq) and Fe(III) in the sediment on the 'cross-shore' transect measured with Au/Hg microelectrode (April 30, 2009). Vertical distributions of O_2 concentration and pH measured with a Clark-type sensor and potentiometric electrode, respectively. Note that profiles with '!!!' were not treated at greater depth for technical reasons ▶

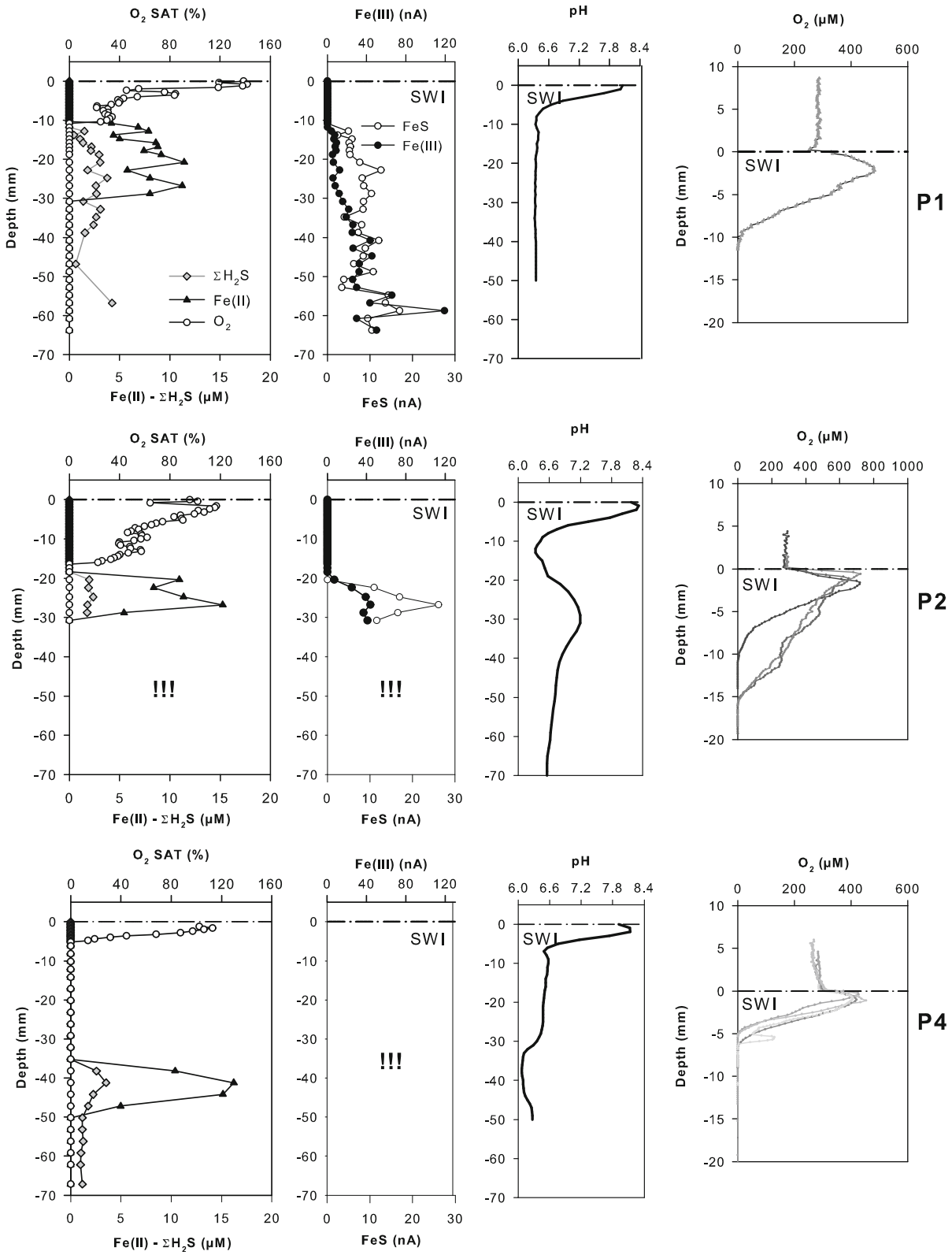
O2 SAT (%)
Fe(III) (nA)
pH
O2 (µM)
Depth (mm)
SWI
ΣH2S
Fe(II)
O2
FeS
Fe(III)
Fe(II) - ΣH2S (µM)
FeS (nA)
!!!
P1
P2
P4

15, 6, 1 and 0.1-μm diamond pastes. The gold disk was plated in a 0.1 M $Hg(NO_3)_2$ solution for 4 min at −0.1 V. The mercury/gold amalgam interface was conditioned at −9 V for 90 s in a 1 N NaOH solution, to strengthen the amalgam between the gold and the mercury. The electrode was then run in linear sweep mode to obtain a reproducible O_2 signal.

The counter electrode was a Pt wire that protruded from the glass tip by 1 to 2 cm. The reference sensor was a glass tube that was flared at one end to receive a small Ag sheet (0.5 × 1 cm), which was soldered to the wire of a coaxial cable and sealed into the glass tip with an epoxy resin (West System). The Ag plate was placed in a hypochlorite solution for several hours to coat the Ag wire/plate with AgCl.

Linear sweep voltammetry (LSV) was used exclusively to measure dissolved oxygen. Square wave voltammetry (SWV) was used to measure Mn(II), Fe(II), and H_2S. Cyclic voltammetry was used to detect $FeS_{(aq)}$ and soluble organic complexes of Fe(III) and H_2S. For all these techniques, the potential was scanned from −0.1 to −1.8 V. To maintain the reproducibility during analysis, a conditioning step can be used between each potential scan. When O_2 was present, conditioning was not necessary. When H_2S or a soluble Fe(III) species were absent, a potential of −0.05 V for 5 s was applied to clean the electrode. When they were present, a potential of −0.9 V was used. Scan rates of 200 mV/s and 1,000 mV/s were applied for SWV and LSV/CV, respectively. Standardization and calibration of the working electrodes are well documented (Brendel & Luther, 1995; Luther et al., 2008).

Water from the site was collected to generate current versus concentration standard curves with standards for each species (Mn(II), Fe(II), H_2S, O_2), and for each electrode. Soluble organic-Fe(III) complexes and $FeS_{(aq)}$ cannot be quantified using external calibrations because a mixture of unknown complexes cannot be calibrated for. (Taillefert et al., 2007). These species are reported as voltammetric current intensities. Voltammetric data were processed using the VOLTINT program software (Bristow & Taillefert, 2008). Average and standard deviations reported represent from three to five measurements at every depth.

Oxygen and pH microprofile measurements

Additional microprofiles of oxygen were measured at 100–200 μm depth increments with Clark-type sensors (Revsbech, 1989) manufactured by Unisense. The sensor tip diameter was 50–100 μm and the 90% response time was shorter than 7 s. Microelectrodes were connected to a high-sensitivity picoammeter (PA2000, Unisense) via an A/D converter. Linear calibrations were done between 100% air saturation in the water at high tide (the oxygen concentration was precisely determined by the Winkler titration), or in the air at low tide, and zero oxygen in the anoxic part of the sediment. Oxygen profiles were processed using the PRO_2FLUX software (Deflandre & Duchene, 2010). Up to six profiles were performed at each site. For documenting the O_2 dynamics in these sediments at low tide, up to 20 profiles were measured between 12:00 and 21:00 at site P3, within a small area of 6 cm^2. Following each profile, the electrode was moved 2–3 cm within a 6 cm^2 zone, in order to avoid artifacts due to modifications of the sediment related to the previous profiles.

Vertical profiles of pH were measured with microelectrodes manufactured by Unisense. The sensor tip diameter was 500 μm and had a response time of less than 60 s. A saturated calomel electrode was used as a reference electrode. Microelectrodes were connected to a high-impedance pH meter (pH-M210, Radiometer) via an A/D converter. Microelectrodes were calibrated according to the protocol SOP6 (Dickson & Goyet, 1996), with two pH standards in a seawater matrix (TRIS and AMP). One pH profile was measured for each site of the cross-shore transect.

These high-resolution measurements of O_2 and pH were conducted at low tide because the equipment was not waterproof. For these measurements, microelectrodes were mounted on a motor controlled micromanipulator (MC-232, Unisense) connected to a PC.

Sediment properties

After in situ measurements, sediment cores were collected during low tide at sites P2, P3, and P4 for the determination of sediment parameters. Cores were sectioned in layers of 5–10 mm. Sub-samples were sealed in preweighed vials and immediately frozen for analysis of the solid fraction. All analyses of the solid sediment were carried out on freeze-dried samples and were corrected for the sea salt content using the measured salinities. The weight lost during freeze-drying was used to calculate water content and sediment porosity (Deflandre et al., 2000, 2002). The

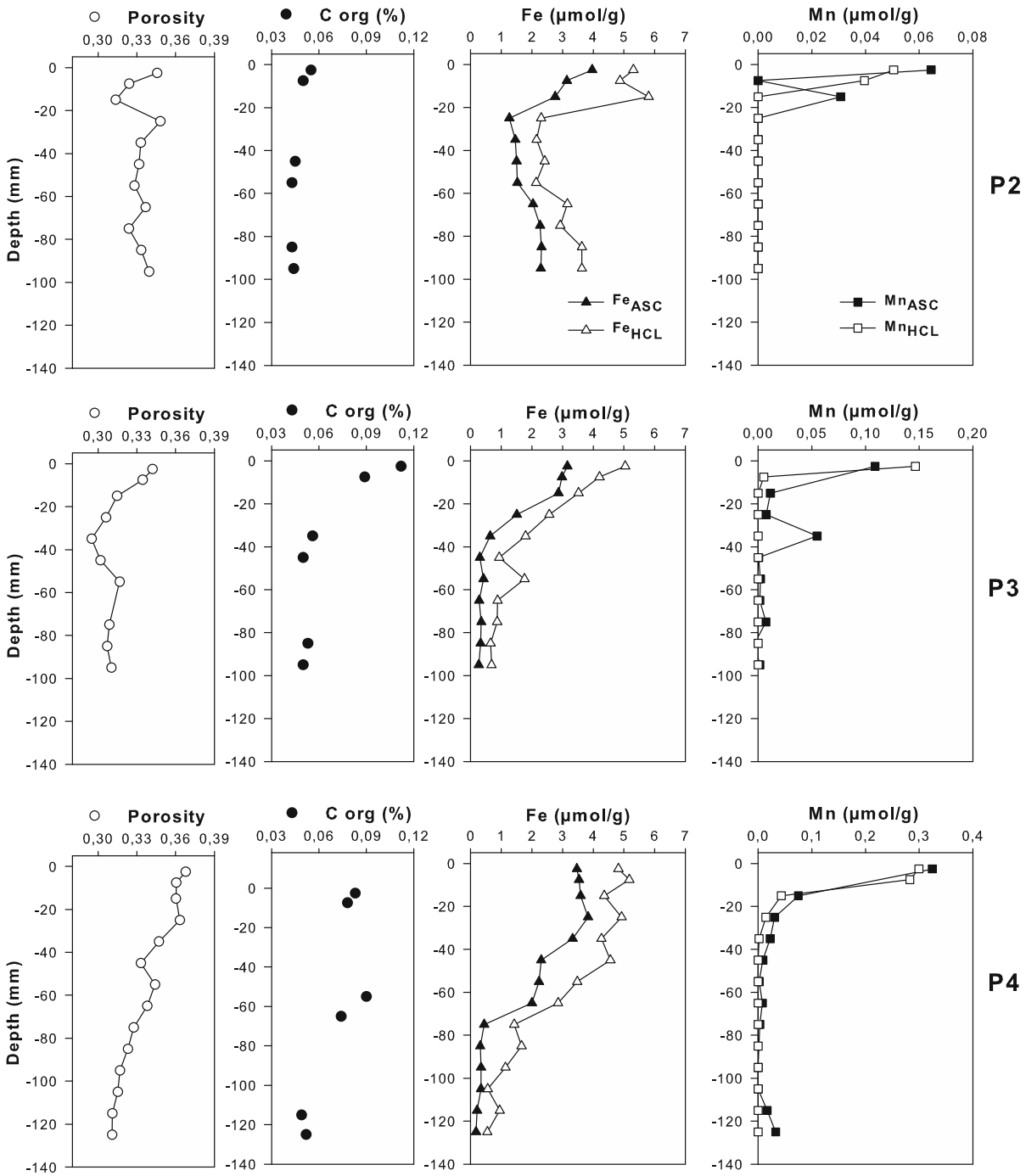

Fig. 3 Depth profiles of porosity, organic carbon, and particulate Fe and Mn extracted by ascorbate and 1 M HCl. Note the different concentration scales for particulate Fe and Mn

freeze-dried samples were homogenized and ground with an agate mortar.

An ascorbate reagent was used to remove the most reactive Fe(III) phases (Fe_{asc}), all Mn(III, IV) oxides and oxyhydroxides (Mn_{asc}), and associated phosphorous (P_{asc}) from the sediment (Kostka & Luther, 1994; Anschutz et al., 1998, 2005). A separate extraction was carried out with 1 M HCl to determine the acid

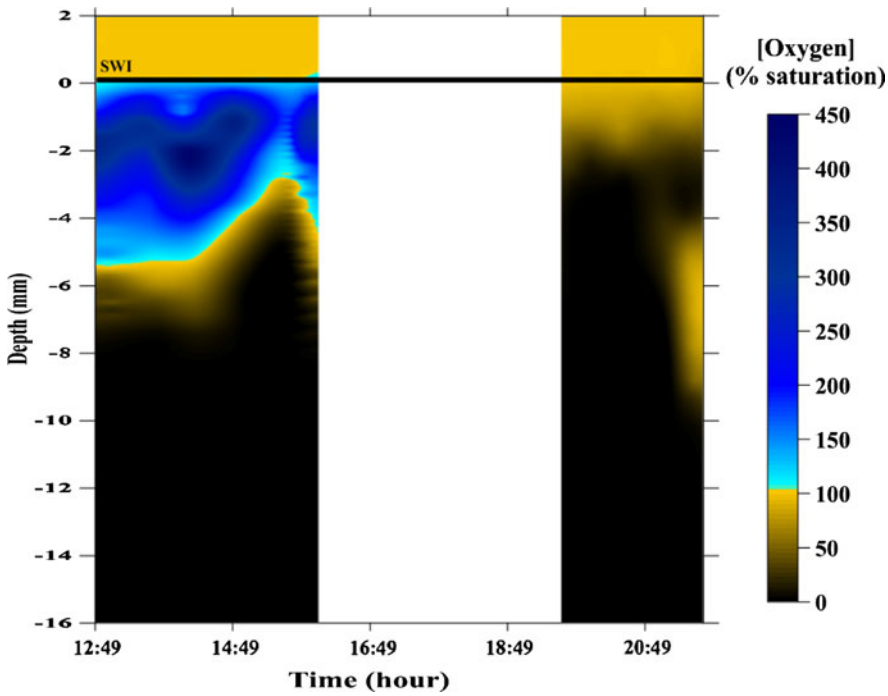

Fig. 4 Temporal evolution of the vertical distribution of O_2 saturation in sediment at site P3 (February 25, 2009). This 2D map was built using the Krigging method with the software Surfer 9 from 12 profiles of dissolved oxygen, which were measured with a Clark-type microelectrode at low tide. The *white rectangle* refers to the period of immersion of the beach when measurements were not performed because the equipment was not waterproof. Note that the weather was nice with no clouds during the experiment

soluble Mn and Fe (Fe_{HCl}, Mn_{HCl}). This reagent was used to dissolve amorphous and crystalline Fe and Mn oxides, carbonates, hydrous aluminum silicates, and associated phosphorous (P_{HCl}) (Kostka & Luther, 1994; Anschutz et al., 2005). For both extractions, 1,000 mg of sample was leached with a 10 ml solution for 24 h, while shaking continuously at room temperature. After each extraction, the samples were centrifuged and the supernatant was analyzed spectrophotometrically for Fe and P (Murphy & Riley, 1962; Stookey, 1970). Flame atomic adsorption spectrometry was used for Mn content determination.

The estimated precision of replicates was ca. 5% for Mn and P, and 7% for Fe. The organic carbon (OC) content was determined from freeze-dried samples with infrared spectroscopy, using a LECO C-S125 gas chromatography analyzer, after removal of carbonates with 2 M HCl. The precision was better than 10%.

Results

Spatial variability of the redox species

Results showed that the sediment profiles of redox species displayed the same global trend at all sites. Oxygen profiles performed with gold amalgam electrodes always displayed an oversaturation of dissolved oxygen under the sediment–water interface, which was associated with a slight increase in pH (Fig. 2). This oversaturation was recovered with better resolution on profiles measured with Clark-type sensors. Then, oxygen was consumed along a more-or-less smooth curve at each site. Oxygen penetration depths (OPD) ranged from 5 to 15 mm with high intra-site variability for P2 and P4. Voltammetric oxygen profiles displayed lower OPD, from 5.2 to 10.8 mm. These observations revealed a high lateral heterogeneity for sediments at cm scale, because the two kinds of sensors were only 10 cm apart.

In the suboxic and anoxic zone, Fe(II) and sulfide appeared successively on the dissolved species profiles (around 20 mm for P2 and 40 mm for P4), whereas iron oxide concentrations decreased (Figs. 2, 3). Deeper in the sediment, Fe(II) disappeared gradually, whereas sulfide concentration increased slightly. At sites P1 and P2, aqueous Fe(III) organic complexes and FeS(aq) appeared with sulfide and Fe(II), and their concentration increased with depth. At site P2, the presence of Fe(III) resulted in a broad signal on voltammograms, which complicated the treatment of the data. None of these species were observed at site P4. Mn(II) was not detected (detection limit of $\sim$15 µM). Dissolved reduced species generally

appeared deeper and in higher concentration along the cross-shore transect (i.e., from P1 to P4) (Fig. 2). In the sediment solid phase, reactive Fe and Mn contents decreased with depth. The thickness of the upper sediment layer, enriched in reactive Fe and Mn, became thicker from P2 to P4, and the stock of Mn increased along the transect.

Temporal evolution of redox species

In situ depth-profile measurements were conducted over time at P3 to determine the effect of tidal forcing on the biogeochemistry of sediment porewaters. The distribution of dissolved oxygen concentration was obtained from a dozen of profiles, measured with a Clark-type microelectrode between 13:00 and 21:00, during the emersion of the beach (Fig. 4). Variations in oxygen concentration occurred on a shorter timescale.

During daylight and before the immersion, an oversaturation of dissolved oxygen was observed in the uppermost layer of the sediment (between the SWI and ~4 mm depth), while the oxygen penetration depth was about 7 mm. After immersion, and during the night, oxygen saturation was 100% at the SWI, decreasing rapidly with depth, down to 2 mm depth. During rising tide, the O_2 concentration started to decrease in the oxic zone greater more than an hour before the arrival of the water. The OPD decreased from 7 to 4 mm during this period, although illumination did not change. At ebb tide, an intrusion of oxygen into the anoxic layer occurred 1 h after the emersion of the beach (Fig. 4).

In situ voltammetric depth-profiles performed over two tidal cycles are presented in Fig. 5. On each profiles, an arrow points the apparition depths of sulfide (ADS). ADS was defined as the depth of the first occurrence of sulfide detection during vertical profiling. ADS was higher at rising tide than at ebb and low tide. Sulfide seemed to appear shallower at the beginning of the immersion than during ebb and low tide. The difference between the ADS at rising and ebb tides was 14 and 8 ± 2.5 mm during the first and second immersion periods studied, respectively.

In situ time-series monitoring of redox species showed that oxygen saturation measured in the overlying water at high tide varied from 100 to 50–60% (Fig. 6). Below the SWI, variations in oxygen saturation at ~7-mm depth showed a similar pattern to those observed previously (Fig. 4). During emersion, the sediment was oversaturated in oxygen during the day and was anoxic overnight. As previously noted, the oxygen saturation decreased just before immersion, with a slight increase in oxygen at the beginning and at the end of immersion. In the anoxic zone, time-series measurements revealed the presence

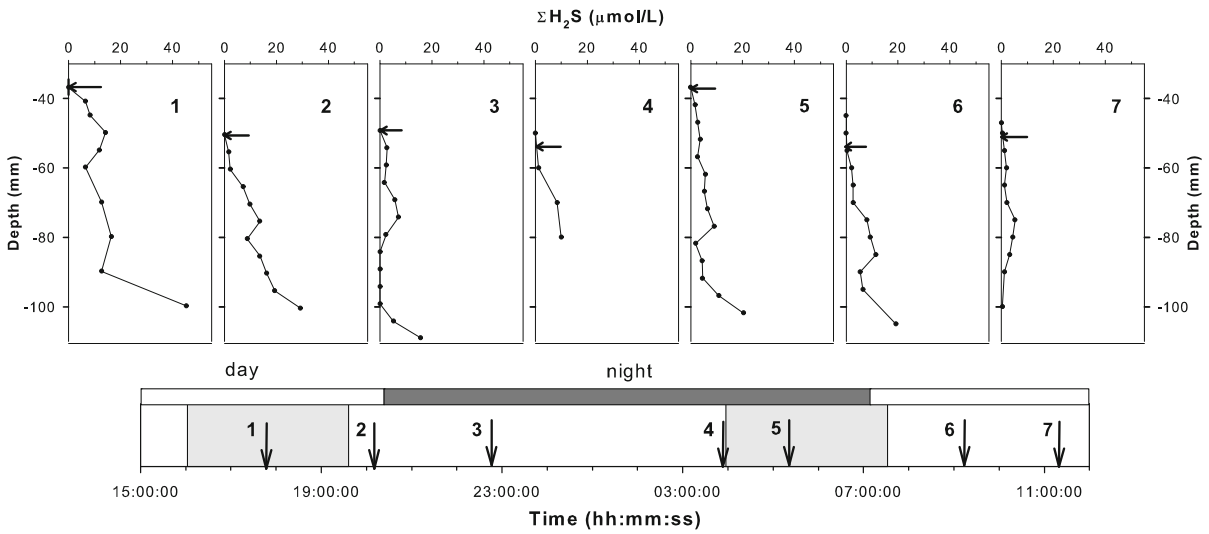

Fig. 5 Temporal evolution of the sulfide appearance depth (*arrow*) estimated from 7 voltammetric in situ profiles, performed during a tidal cycle at station P3 (April 7–8, 2009). *Gray zones* refer to periods of immersion of the beach. Note that the weather was nice with no clouds during the experiment

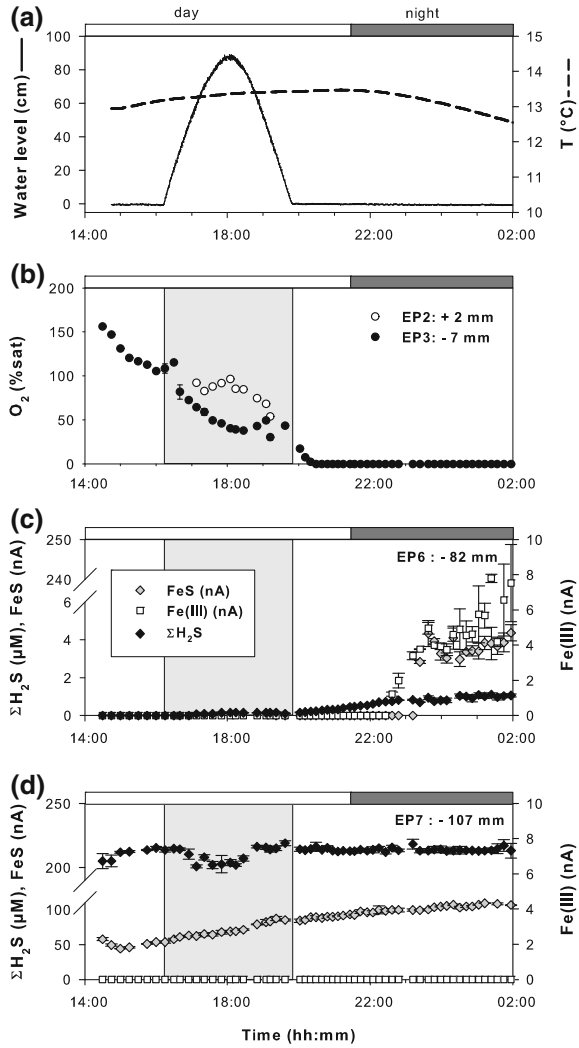

Fig. 6 **a** Water level and temperature measured in a monitoring well by a pressure transducer. Temporal evolution of O_2, ΣH_2S, $FeS_{(aq)}$, and Fe(III) measured in situ between 14:00 and 2:00 (April 8–9, 2009), with solid-state Au/Hg microelectrodes located at 4 different depths: **b** +2 mm and −7 mm, **c** −82 mm, **d** −107 mm. The Gray zone indicates the period of immersion of the beach. Mn(II) was below the detection limit (i.e., ∼15 µM). Note that the weather was nice with no clouds during the experiment

of dissolved sulfide, soluble organic-Fe(III), and $FeS_{(aq)}$.

At 107 mm depth, soluble FeS did not show a significant relationship with tidal or diurnal cycles. Sulfide concentration was relatively constant until rising tide when it decreased from 215 to 200 µM during more than an hour before returning to its initial value. This decrease occurred simultaneously with the appearance of sulfide at a detectable concentration at 82 mm depth. At this depth, sulfide increased slightly until 22:00, to a constant value of 1 µM. At that time, soluble FeS and organic-Fe(III) became detectable and increased up to 5 nA. At rising tide, sulfide was slightly removed at depth, and appeared simultaneously nearer the SWI.

Discussion

The vertical distribution of redox species

Depth-profiles along the cross-shore transect (Figs. 2, 3) reflect aerobic and anaerobic microbial activities. An oversaturation of oxygen under the SWI is typically associated with the photosynthetic activity of microphytobenthos (e.g., Epping et al., 1999), which produces O_2 and consumes protons, causing a slight increase in pH as observed in Fig. 2. Below the photosynthetic layer, profiles of redox compounds reflect benthic processes of organic matter mineralization. Oxygen was depleted within the first 15 mm (between 5 mm at P4 and 15 mm at P2) below the

sediment–water interface. Oxic respiration was restricted, therefore, to the upper 5–15 mm. Oxygen microprofiles measured with Clark-type sensors showed evidence of burrow irrigation at P2 and P4 (Fig. 2). The influence of faunal activity was also apparent in the overnight hours through the continuous recording carried out at site P3 (Fig. 4). The sediments of the Arcachon Bay mud flat are densely populated (>20,000 ind m^{-2}) by annelids and bivalves (Blanchet et al., 2004).

Below the oxic layer, anaerobic processes took place, with the reduction of manganese oxides, iron oxides, and sulfate according to the well-established processes of anaerobic organic matter mineralization described by Froelich et al. (1979). This led to the observed decrease in particulate Fe and Mn extracted with ascorbate, and an accumulation of Fe(II) and ΣH_2S in the sediment porewater. Dissolved Mn(II) was not detected, likely because of the high detection limit of the voltammetric electrode and the low content of Mn in the sediment solid phase. Secondary redox reactions may have occurred between the products of primary respiration reactions (e.g., Fe(II) and ΣH_2S). Precipitation of Fe(II) with ΣH_2S is evidenced by the presence of $FeS_{(aq)}$, which is an intermediate in pyrite formation (Theberge & Luther, 1997; Bull & Taillefert, 2001).

Oxidation of Fe(II) by hydrous iron oxides may produce soluble organic-Fe(III) in the presence of organic ligand when oxygen is not available. This reaction was studied at a pH <6 (Sulzberger et al., 1989; Suter et al., 1991), and it occurred presumably in acidic conditions only (Pronk & Johnson, 1992). However, the pH was always greater than 6 in the sediment porewater of the study area, which does not favor such a reaction. As soluble organic-Fe(III) can be found together with Fe(II), Taillefert et al. (2002) proposed that this organic compound could be an intermediate in the bacterial reduction of solid Fe(III), or could be formed by oxidation of organic-Fe(II) complexes.

The depth of the initial appearance of dissolved Fe(II) and ΣH_2S increased between P1 and P4. This depth was always several mm below the OPD, which suggests that the primary oxidant for these compounds was not oxygen. Alternative oxidants may be nitrate, not measured here, or particulate Mn oxides (Hyacinthe et al., 2001), which were detected deeper at P4 than at P1.

As expected in a coastal sediment, profiles were different from a site to another along the cross-shore transect. Differences were likely due to spatial and temporal changes. Dissolved species profiles were conducted between 10:45 and 21:00 from site 1 to site 4. Over this measurement period, environmental parameters such as luminosity and water level evolved. We observed also that the porosity increased from P1 to P4, reflecting probably variation in mud content of the sediment along the transect (Fig. 3). However, the relative distribution of redox compounds was qualitatively homogenous in all site studied, so that mechanisms inducing temporal evolution of the sediment biogeochemistry are expected to be qualitatively homogenous as well.

Short-term evolution of redox species in the Arcachon lagoon sediments

The short-term variability of redox species sediment was studied over a complete tidal cycle at site P3, but processes encountered at this site could be generalized to that of the other sites. In situ depth-profiles and time-series highlight the short-term variability of redox species associated with tidal and daylight changes (Figs. 4, 5, 6). Therefore, the profiles of the cross-shore transect discussed in the previous section were only instantaneous pictures of transient distributions of dissolved species. The tides induced modifications of hydrostatic pressure in the sediment that may lead to porewater transport (Billerbeck et al., 2006b; Taillefert et al., 2007; Deborde et al., 2008b). Transport of interstitial fluid may influence biological processes, and thus may modify the spatial distribution of redox species over time. This is particularly true in permeable sediments for which advective transport processes become significant once permeability exceeds 10^{-12} m^2 (Huettel et al., 1998; Boudreau & Jørgensen, 2001). The studied sediment has a permeability of 1.2×10^{-11} m^2. Therefore, the porewater flow resulting from the tidal forcing may induce transport of dissolved and suspended matter in the interstitial space. We observed, however, that the sediment surface remained water-saturated during emersion. This suggests that vertical movements of pore water were hindered during this period, probably because of the low slope of the beach. It is also possible that downward transport due to pressure gradient occurs during emersion, but the capillary

forces may counteract the hydrostatic force so that sediments remain water-saturated.

Linking tidal dynamics of oxygen with the microphytobenthic production

The oxygen dynamics at site P3 displayed temporal variations related to the diurnal cycle (Figs. 4, 6). The variations in irradiance influence the production by microphytobenthos, and the subsequent oxygen dynamics (Epping and Jørgensen, 1996; Bartoli et al., 2003). During day and night, this photosynthetic production and the anaerobic respiration controlled alternatively the oxygen saturation in the sediment.

Some variations of oxygen concentration are linked to the tidal cycles. At rising tide, the benthic oxygen saturation decreased right before inundation (Fig. 4). Similarly, Spilmont et al. (2007) and Migné et al. (2009) have previously observed that benthic primary production deduced from CO_2 uptake started to decrease about 100 min before the immersion of a muddy sand flat in the bay of Somme (eastern English Channel, France) while irradiance was still increasing. Numerous studies indicated the possibility of a vertical migration of microphytobenthos in intertidal mudflats (Round & Palmer, 1966; Serôdio et al., 1997; Serôdio & Catarino, 2000), and intertidal sandy sediments (Easley et al., 2005; Jesus et al., 2009). Cells may migrate into deeper sediment before the incoming tide, resulting in a drastic decrease of the photosynthetic production. An upward movement of microalgae to the surface may occur during ebb tide. This migratory rhythm is endogenous, but the determinism of this behavior is not yet well understood (Serôdio et al., 1997; Guarini et al., 2000). The migration of microphytobenthos influences the photosynthetic production, which becomes limited by light (Walpersdorf et al., 2009). This phenomenon has likely caused the monitored diminution of the oxygen saturation in the sediment (Fig. 6).

At the beginning and at the end of the sand flat inundation, small increases in oxygen occurred at 7 mm depth (Fig 6). The tidal flushing and the currents moving over ripples, particularly, may have driven oxygenated water from the water column into the permeable sediments and may, therefore, explain these little variations of oxygen saturation (Huettel et al., 1998; De Beer et al., 2005; Billerbeck et al., 2006b; Jansen et al., 2009).

During the night, oxygen appeared below the SWI in deeper zones, which were typically anoxic (Fig. 4). This suggests that the sensor crossed ventilated burrows. The occurrence of subsurface oxygen peaks showed that the animals in the burrows were actively pumping oxygen down for their respiration (Jørgensen et al., 2005).

Influence of the tidal pump on the behavior of reduced species

In situ high-resolution time-series of reduced dissolved species reported here gives original information on the transient biogeochemistry of an intertidal sandy sediment. This unique data set enables characterization of the short-term variability of the distribution of reduced species throughout the tidal and the diurnal cycles. Time-series at 107- and 82-mm depth showed a different evolution for dissolved sulfide (Fig. 6). At 107 mm, the concentration remained high and constant during the whole monitoring except a small jump during the emersion of the studied beach when sulfide concentration increased at 82 mm and decreased at 107 mm. This suggests that an oscillation of the redox front occurred at high tide. At 82 mm, variations of reduced species concentrations were mainly linked to the diurnal cycle. During the night, oxygen was probably consumed rapidly resulting in a thinning down of the oxic layer and thus in an upward migration of reduced species. However, we cannot explain the simultaneous increase in soluble organic-Fe(III). The high concentration gradient between 8 (<1 μM) and 10 (<200 μM) cm depth suggests that sulfides may be retained in deep layers of the sediment. During emersion, results suggest that this sulfide gradient is quite smaller than at low tide. The concentration gradient generates transport through molecular diffusion. The propagation of a gradient by diffusive processes occurs according to the Einstein-Smolouchowski equation (Boudreau, 1996: $x^2 = 2tD_s$, where x is distance, t is time, and D_s is the diffusion coefficient in the sediment porewater). The time required to move the sulfide gradient by molecular diffusion over 2 cm is on the order of 5 days (using $D_s = 0.45 \times 10^{-5}$ cm^2 s^{-1} for H_2S at 12.5°C and a porosity of 0.33; Schulz & Zabel, 2006). Therefore, diffusive transport alone cannot explain the variation of the sulfide concentration gradient during high tide. In the studied area, it has been shown

that porewaters seeped through the sediment, into channel waters during ebb tide, draining tidal flats (Deborde et al., 2008b). This flow of interstitial water toward the seepage zone is generated at ebb tide by a hydraulic gradient, resulting in an elevation difference between the porewater level in the upper sand flat and the water level in the tidal channel (Nielsen, 1990; Billerbeck et al., 2006a, b; Jansen et al., 2009). This seep transport may explain why sulfides could not penetrate the upper layers of sediment, resulting in the concentration gradient of sulfides between 10 and 8 cm depth. At rising tide, the pressure head is reversed and the sulfide-containing porewaters may migrate toward the surface sediments resulting in a quite smaller sulfide concentration gradient. However, further investigations are needed to make any conclusion about the mechanism that may explain such results. Data on sulfide concentration above and below 107 mm would help us to conclude.

Profiles measured in situ the day before the time-series monitoring at the same site also showed variations that may be linked to tidal cycles. The depth of initial sulfide appearance oscillated between 35 mm at the beginning of immersion and 55 mm at the end of immersion and during emersion (Fig. 5). At rising tide, sulfides seemed to migrate toward the SWI (Fig. 5) as suggested with results previously presented. Taillefert et al. (2007) also suggested that an advection of porewater at rising tide might push sulfides toward the SWI. However, this migration is not clear and profiles with larger depth and higher resolution should be performed in a future study.

The two different data sets suggest that the vertical distribution of sulfide may oscillate with tides. However, these data obtained on the same site during two consecutive days with two different methodological approaches are not consistent on some points. Sulfide was not detected at 8 cm in the time-series but it appeared at least at 5 cm depth in all the profiles. In addition, sulfide concentrations measured at 10 cm depth in time-series does not match with those measured at this depth in the profiles. These results from both approaches clearly showed that tidal cycles influence the vertical distribution of redox species. Differences between the two data sets showed that this influence is not necessarily cyclic even though an effect of the sediment heterogeneity cannot be excluded. We need further investigations and longer time-series to give a mechanistic explanation of how tides induce redox front oscillations and change the porewater chemistry.

Conclusion

Tidal environments are transient. In situ voltammetry is a very promising technique to describe the short-term evolution of major redox components without sampling artifacts allowing to understand how redox reactions evolve with the tidal and day–night cycles. In addition, this innovative approach also enabled to observe in situ and in real-time the vertical migration of microphytobenthos from continuous measurements of oxygen saturation. Such monitoring may provide, in the future, new data for describing the consequences of various types of natural and anthropogenic forcing on coastal ecosystems. This is particularly important in the Arcachon lagoon where the sediment biogeochemistry must be constrained because of the present-day context of decrease in the *Zostera noltii* meadow surface (Dalloyau et al., 2009; Plus et al., 2010). The effect of tides on the biogeochemistry of intertidal sediments depends on sediment permeability, topography of the flat, hydrodynamics (waves and currents), and the activities of microphytobenthos. Variations in these factors can generate opposite effects on the dynamics of redox species, such as oxygen or sulfides. Further investigations are needed to determine which of these factors are dominant in the Arcachon Bay sediments.

Acknowledgments We thank Dr. Henri Etcheber for particulate organic carbon analysis, Pr. Gérard Blanc and Dr. Jörg Schäfer for the access to the flame atomic adsorption spectrometer. Special thanks to the city of Lanton-Cassy and their help during this work. We also gratefully acknowledge Georges Oggian, Hervé Derriennic, Dominique Poirier, Vincent Hanquiez, and Marie Wawrzykowski for helpful support in the field and with sample analysis. This study was supported by the French National Research Agency ("ANR Blanche") program Protidal, and the French INSU-EC2CO/PNEC program MOBISEA. M. L. D. received a special grant from la Région Réunion.

References

Anschutz, P., S. Zhong, B. Sundby, A. Mucci & C. Gobeil, 1998. Burial efficiency of phosphorus and the geochemistry of iron in continental margin sediments. Limnology and Oceanography 43: 53–64.

Anschutz, P., K. Dedieu, F. Desmazes & G. Chaillou, 2005. Speciation, oxidation state, and reactivity of particulate

manganese in marine sediments. Chemical Geology 218: 265–279.

Azzoni, R., G. Giordani, M. Bartoli, D. T. Welsh & P. Viaroli, 2001. Iron, sulphur and phosphorus cycling in the rhizosphere sediments of a eutrophic Ruppia cirrhosa meadow (Valle Smarlacca, Italy). Journal of Sea Research 45: 15–26.

Bartoli, M., D. Nizzoli & P. Viaroli, 2003. Microphytobenthos activity and fluxes at the sediment-water interface: interactions and spatial variability. Aquatic Ecology 37: 341–349.

Beck, M., O. Dellwig, G. Liebezeit, B. Schnetger & H. J. Brumsack, 2008. Spatial and seasonal variations of sulphate, dissolved organic carbon, and nutrients in deep pore waters of intertidal flat sediments. Estuarine, Coastal and Shelf Science 79: 307–316.

Billerbeck, M., U. Werner, K. Bosselmann, E. Walpersdorf & M. Huettel, 2006a. Nutrient release from an exposed intertidal sand flat. Marine Ecology Progress Series 316: 35–51.

Billerbeck, M., U. Werner, L. Polerecky, E. Walpersdorf, D. DeBeer & M. Huettel, 2006b. Surficial and deep pore water circulation governs spatial and temporal scales of nutrient recycling in intertidal sand flat sediment. Marine Ecology Progress Series 326: 61–76.

Blanchet, H., X. De Montaudouin, A. Lucas & P. Chardy, 2004. Heterogeneity of macrozoobenthic assemblages within a *Zostera noltii* seagrass bed: diversity, abundance, biomass and structuring factors. Estuarine, Coastal and Shelf Science 61: 111–123.

Böttcher, M. E., B. Hespenheide, E. Llobet-Brossa, C. Beardsley, O. Larsen, A. Schramm, A. Wieland, G. Böttcher, U. G. Berninger & R. Amann, 2000. The biogeochemistry, stable isotope geochemistry, and microbial community structure of a temperate intertidal mudflat: an integrated study. Continental Shelf Research 20: 1749–1769.

Boudreau, B. P., 1996. The diffusive tortuosity of fine-grained unlithified sediments. Geochimica et Cosmochimica Acta 60: 3139–3142.

Boudreau, B. P. & B. B. Jørgensen, 2001. The Benthic Boundary Layer. Oxford University Press, Oxford: 440 pp.

Brendel, P. J. & G. W. Luther, 1995. Development of a gold amalgam voltammetric microelectrode for the determination of dissolved Fe, Mn, O_2, and S(−II) in porewaters of marine and freshwater sediments. Environmental Science and Technology 29: 751–761.

Bristow, G. & M. Taillefert, 2008. VOLTINT: a Matlab®-based program for semi-automated processing of geochemical data acquired by voltammetry. Computers & Geosciences 34: 153–162.

Bull, D. C. & M. Taillefert, 2001. Seasonal and topographic variations in porewaters of a southeastern USA salt marsh are revealed by voltammetric profiling. Geochemical Transactions 2: 104–111.

Canton, M., P. Anschutz, V. Naudet, D. Poirier, F. Naessens, M. Francecshi, N. Molnar & A. Mouret, 2010. Impact of a solid waste disposal on nutrient dynamics in a sandy catchment. Journal of Contaminant Hydrology 116: 1–15.

Dalloyau, S., G. Trut, M. Plus & I. Auby, 2009. Caractérisation de la qualité biologique des Masses d'Eau Côtières: Cartographie des herbiers de *Zostera noltii* et *Zostera marina* du Bassin d'Arcachon. Rapport Ifremer: 52 pp.

De Beer, D., F. Wenzhöfer, T. G. Ferdelman, S. E. Boehme, M. Huettel, J. E. E. Van Beusekom, M. E. Böttcher, N. Musat & N. Dubilier, 2005. Transport and mineralization rates in North Sea sandy intertidal sediments, Sylt-Rømø Basin, Wadden Sea. Limnology and Oceanography 50: 113–127.

De Wit, R., L. J. Stal, B. A. Lomstein, R. A. Herbert, H. van Gemerden, P. Viaroli, V.-U. Cecherelli, F. RodrÌguez-Valera, M. Bartoli, G. Giordani, R. Azzoni, B. Schaub, D. T. Welsh, A. Donnelly, A. Cifuentes, J. AntÛn, K. Finster, L. B. Nielsen, A.-G. U. Pedersen, A. T. Neubauer, M. A. Colangelo & S. K. Heijs, 2001. ROBUST: the ROle of BUffering capacities in STabilising coastal lagoon ecosystems. Continental Shelf Research 21: 2021–2041.

Deborde, J., G. Abril, A. Mouret, D. Jézéquel, G. Thouzeau, J. Clavier, G. Bachelet & P. Anschutz, 2008a. Effects of seasonal dynamics in a *Zostera noltii* meadow on phosphorus and iron cycles in a tidal mudflat (Arcachon Bay, France). Marine Ecology Progress Series 355: 59–71.

Deborde, J., P. Anschutz, I. Auby, C. Glé, M. V. Commarieu, D. Maurer, P. Lecroart & G. Abril, 2008b. Role of tidal pumping on nutrient cycling in a temperate lagoon (Arcachon Bay, France). Marine Chemistry 109: 98–114.

Deflandre, B. & J. C. Duchene, 2010. PRO2FLUX: a software for PRofile quantification and diffusive O_2 FLUX calculation. Environmental Modelling & Software 25: 1059–1061.

Deflandre, B., J.-P. Gagné, B. Sundby, A. Mucci, C. Guignard & P. Anschutz, 2000. The 1996 flood event: disruption of the ongoing diagenesis of Saguenay Fjord sediments. Proceeding for the Canadian Geotechnical Society 1: 117–122.

Deflandre, B., A. Mucci, J. P. Gagné, C. Guignard & B. Sundby, 2002. Early diagenetic processes in coastal marine sediments disturbed by a catastrophic sedimentation event. Geochimica et Cosmochimica Acta 66: 2547–2558.

Dickson, A. G. & C. Goyet, 1996. SOP6: determination of the pH of sea water using a glass/reference electrode cell. In Dickson, A. G. & C. Goyet (eds), Handbook of Methods for the Analysis of the Various Parameters of the Carbon Dioxide System in Sea Water, Version 2.1. ORNL/CDIAC-74.

Easley, J. T., S. N. Hymel & C. J. Plante, 2005. Temporal patterns of benthic microalgal migration on a semi-protected beach. Estuarine, Coastal and Shelf Science 64: 486–496.

Epping, E. H. G. & B. B. Jørgensen, 1996. Light enhanced oxygen respiration in benthic phototrophic communities. Marine Ecology Progress Series 139: 193–203.

Epping, E. H. G., A. Khalili & R. Thar, 1999. Photosynthesis and the dynamics of oxygen consumption in a microbial mat as calculated from transient oxygen microprofiles. Limnology and Oceanography 44: 1936–1948.

Falkowski, P. G., R. T. Barber & V. Smetacek, 1998. Biogeochemical controls and feedbacks on ocean primary production. Science 281: 200–206.

Froelich, P. N., G. P. Klinkhammer, M. L. Bender, N. A. Luedtke, G. R. Heath, D. Cullen, P. Dauphin, D. Hammond, B. Hartman & V. Maynard, 1979. Early oxidation of organic matter in pelagic sediments of the eastern equatorial Atlantic: suboxic diagenesis. Geochimica et Cosmochimica Acta 43: 1075–1090.

Gassiat L., 1989. Hydrodynamique et évolution sédimentaire d'un système lagune-flèche littorale: le Bassin d'Arcachon et la flèche du Cap Ferret. Ph.D. dissertation, Université Bordeaux I: 340 pp.

Guarini, J. M., G. F. Blanchard & P. Gros, 2000. Quantification of the microphytobenthic primary production in European intertidal mudflats: a modelling approach. Continental Shelf Research 20: 1771–1788.

Huettel, M., W. Ziebis, S. Forster & G. W. Luther III, 1998. Advective transport affecting metal and nutrient distributions and interfacial fluxes in permeable sediments. Geochimica et Cosmochimica Acta 62: 613–631.

Hyacinthe, C., P. Anschutz, P. Carbonel, J. M. Jouanneau & F. J. Jorissen, 2001. Early diagenetic processes in the muddy sediments of the Bay of Biscay. Marine Geology 177: 111–128.

Jahnke, R. A., C. R. Alexander & J. E. Kostka, 2003. Advective pore water input of nutrients to the Satilla River Estuary, Georgia, USA. Estuarine, Coastal and Shelf Science 56: 641–653.

Jansen, S., E. Walpersdorf, U. Werner, M. Billerbeck, M. E. Böttcher & D. De Beer, 2009. Functioning of intertidal flats inferred from temporal and spatial dynamics of O_2, H_2S and pH in their surface sediment. Ocean Dynamics 59: 317–332.

Jesus, B., V. Brotas, L. Ribeiro, C. R. Mendes, P. Cartaxana & D. M. Paterson, 2009. Adaptations of microphytobenthos assemblages to sediment type and tidal position. Continental Shelf Research 29: 1624–1634.

Jørgensen, B. B., R. N. Glud & O. Holby, 2005. Oxygen distribution and bioirrigation in Arctic fjord sediments (Svalbard, Barents Sea). Marine Ecology Progress Series 292: 85–95.

Kostka, J. E. & G. W. Luther, 1994. Partitioning and speciation of solid phase iron in saltmarsh sediments. Geochimica et Cosmochimica Acta 58: 1701–1710.

Luther III, G. W., C. E. Reimers, D. B. Nuzzio & D. Lovalvo, 1999. In situ deployment of voltammetric, potentiometric, and amperometric microelectrodes from a ROV to determine dissolved O_2, Mn, Fe, S(−II), and pH in porewaters. Environmental Science and Technology 33: 4352–4356.

Luther III, G. W., B. T. Glazer, L. Hohmann, J. I. Popp, M. Taillefert, T. F. Rozan, P. J. Brendel, S. M. Theberge & D. B. Nuzzio, 2001. Sulfur speciation monitored in situ with solid state gold amalgam voltammetric microelectrodes: polysulfides as a special case in sediments, microbial mats and hydrothermal vent waters. Journal of Environmental Monitoring 3: 61–66.

Luther III, G. W., B. T. Glazer, S. Ma, R. E. Trouwborst, T. S. Moore, E. Metzger, C. Kraiya, T. J. Waite, G. Druschel, B. Sundby, M. Taillefert, D. B. Nuzzio, T. M. Shank, B. L. Lewis & P. J. Brendel, 2008. Use of voltammetric solid-state (micro)electrodes for studying biogeochemical processes: laboratory measurements to real time measurements with an in situ electrochemical analyzer (ISEA). Marine Chemistry 108: 221–235.

Migné, A., N. Spilmont, G. Boucher, L. Denis, C. Hubas, M. A. Janquin, M. Rauch & D. Davoult, 2009. Annual budget of benthic production in Mont Saint-Michel Bay considering cloudiness, microphytobenthos migration, and variability of respiration rates with tidal conditions. Continental Shelf Research 29: 2280–2285.

Murphy, J. & J. P. Riley, 1962. A modified single solution method for the determination of phosphate in natural waters. Analytica Chimica Acta 27: 31–36.

Nielsen, P., 1990. Tidal dynamics of the water table in beaches. Water Resources Research 26: 2127–2134.

Nielsen, L. B., K. Finster, D. T. Welsh, A. Donelly, R. A. Herbert, R. De Wit & B. A. A. Lomstein, 2001. Sulphate reduction and nitrogen fixation rates associated with roots, rhizomes and sediments from *Zostera noltii* and *Spartina maritima* meadows. Environmental Microbiology 3: 63–71.

Plus, M., S. Dalloyau, G. Trust, I. Auby, X. de Montaudouin, E. Emery, C. Noël & C. Viala, 2010. Long-term evolution (1988–2008) of *Zostera* spp. meadows in Arcachon Bay (Bay of Biscay). Estuarine, Coastal and Shelf Science 87: 357–366.

Pringault, O., R. de Wit & M. Kühl, 1999. A microsensor study of the interaction between purple sulfur and green sulfur bacteria in experimental benthic gradients. Microbial Ecology 34: 173–184.

Pronk, J. T. & D. B. Johnson, 1992. Oxidation and reduction of iron by acidophilic bacteria. Geomicrobiology Journal 10: 153–171.

Rauch, M. & L. Denis, 2008. Spatio-temporal variability in benthic mineralization processes in the eastern English Channel. Biogeochemistry 89: 163–180.

Reimers, C. E., H. A. Stecher, G. L. Taghon, C. M. Fuller, M. Huettel, A. Rusch, N. Ryckelynck & C. Wild, 2004. In situ measurements of advective solute transport in permeable shelf sands. Continental Shelf Research 24: 183–201.

Revsbech, N. P., 1989. An oxygen microsensor with a guard cathode. Limnology and Oceanography 34: 474–478.

Rimmelin, P., J. C. Dumon, E. Maneux & A. Gonçalves, 1998. Study of annual and seasonal dissolved inorganic nitrogen inputs into the Arcachon Lagoon, Atlantic Coast (France). Estuarine, Coastal and Shelf Science 47: 649–659.

Rocha, C., 1998. Rhythmic ammonium regeneration and flushing in intertidal sediments of the Sado estuary. Limnology and Oceanography 43: 823–831.

Rocha, C. & P. Cabral, 1998. The influence of tidal action on porewater nitrate concentration and dynamics in intertidal sediments of the Sado Estuary. Estuaries 21: 635–645.

Round, F. E. & J. D. Palmer, 1966. Persistent, vertical-migration rhythms in benthic microflora. II. Field and laboratory studies on diatoms from the banks of the River Avon. Journal of the Marine Biological Association of the UK 46: 191–214.

Roy, H., S. L. Jae, S. Jansen & D. De Beer, 2008. Tide-driven deep pore-water flow in intertidal sand flats. Limnology and oceanography 53: 1521–1530.

Rusch, A. & M. Huettel, 2000. Advective particle transport into permeable sediments: evidence from experiments in an intertidal sandflat. Limnology and Oceanography 45: 525–533.

Rusch, A., M. Huettel & S. Forster, 2000. Particulate organic matter in permeable marine sands: dynamics in time and depth. Estuarine, Coastal and Shelf Science 51: 399–414.

Rusch, A., S. Forster & M. Huettel, 2001. Bacteria, diatoms and detritus in an intertidal sandflat subject to advective

transport across the water-sediment interface. Biogeochemistry 55: 1–27.

Schulz, H. D. & M. Zabel, 2006. Marine Geochemistry. Springer, Berlin: 575 pp.

Serôdio, J. & F. Catarino, 2000. Modelling the primary productivity of intertidal microphytobenthos: time scales of variability and effects of migratory rhythms. Marine Ecology Progress Series 192: 13–30.

Serôdio, J., J. M. Da Silva & F. Catarino, 1997. Nondestructive tracing of migratory rhythms of intertidal benthic microalgae using in vivo chlorophyll *a* fluorescence. Journal of Phycology 33: 542–553.

Spilmont, N., A. Migné, L. Seuront & D. Davoult, 2007. Short-term variability of intertidal benthic community production during emersion and the implication in annual budget calculation. Marine Ecology Progress Series 333: 95–101.

Stookey, L. L., 1970. Ferrozine: a new spectrophotometric reagent for iron. Analytical Chemistry 42: 779–781.

Sulzberger, B., D. Suter, C. Siffert, S. Banwart & W. Stumm, 1989. Dissolution of fe(III)(hydr)oxides in natural waters; laboratory assessment on the kinetics controlled by surface coordination. Marine Chemistry 28: 127–144.

Suter, D., S. Banwart & W. Stumm, 1991. Dissolution of hydrous iron(III) oxides by reductive mechanisms. Langmuir 7: 809–813.

Taillefert, M., G. W. Luther III & D. B. Nuzzio, 1999. The application of electrochemical tools for in situ measurements in aquatic systems. Electroanalysis 12: 401–412.

Taillefert, M., V. C. Hover, T. F. Rozan, S. M. Theberge & G. W. Luther, 2002. The influence of sulfides on soluble organic-Fe(III) in anoxic sediment porewaters. Estuaries 25: 1088–1096.

Taillefert, M., S. Neuhuber & G. Bristow, 2007. The effect of tidal forcing on biogeochemical processes in intertidal salt marsh sediments. Geochemical Transactions 8: 6.

Theberge, S. M. & G. W. Luther, 1997. Determination of the electrochemical properties of a soluble aqueous FeS species present in sulfidic solutions. Aquatic Geochemistry 3: 191–211.

Viaroli, P., M. Bartoli, C. Bondavalli, R. R. Christian, G. Giordani & M. Naldi, 1996. Macrophyte communities and their impact on benthic fluxes of oxygen, sulphide and nutrients in shallow eutrophic environments. Hydrobiologia 329: 105–119.

Walpersdorf, E., U. Werner, L. Polerecky, U. Franke, P. Bird & D. De Beer. Tidal dynamics of O_2, H_2S and pH in permeable sands. In ASLO 2009 Meeting, January 25–30, 2009, Nice, France.